Journal of Sedimentary Research

Journal of Sedimentary Research, 2014, v. 84, 825–836
Research Article
DOI: http://dx.doi.org/10.2110/jsr.2014.60

PALEOSLOPE RECONSTRUCTION IN SANDY SUSPENDED-LOAD-DOMINANT RIVERS

RANIE M. LYNDS,[1] DAVID MOHRIG,[2] ELIZABETH A. HAJEK,[3] AND PAUL L. HELLER[4]

[1]*Wyoming State Geological Survey, P.O. Box 1347, Laramie, Wyoming 82073, U.S.A.*
[2]*Department of Geological Sciences, The University of Texas at Austin, 1 University Station C9000, Austin, Texas 78712, U.S.A.*
[3]*Department of Geosciences, Pennsylvania State University, 511 Deike Building, University Park, Pennsylvania 16802, U.S.A.*
[4]*Department of Geology and Geophysics, University of Wyoming, 1000 East University Avenue, Department 3006, Laramie, Wyoming 82071, U.S.A.*
e-mail: ranie.lynds@wyo.gov

ABSTRACT: **Constraining the depositional gradient of ancient alluvial river systems can aid in reconstructing landscapes and estimating paleodischarge by establishing boundaries on the climatic and tectonic history of continental sequences. We present three methods for estimating ancient depositional gradients based on the interpreted mode of sediment transport for the range of particle sizes found on the beds of modern rivers or preserved in channel fills. For sandy rivers with suspension as the dominant mode of sediment transport, these methods take advantage of observations that can be directly obtained from preserved strata, including measurements of paleo flow depth and grain size. The first method relates river slope to Shields number at bankfull flow. The second method is similar to the first but allows for variation in Shields number at bankfull flow with grain diameter. The final method relies on criteria required for both suspended- and bed-material load sediment transport in the same system and is the most comprehensive and physically justified method. We present each method and test them with modern river datasets to verify accuracy and help constrain uncertainty—the first step to adapting them to ancient systems. Results indicate that all methods estimate slope within a factor of two. These methods are potentially very powerful for interpreting sandy fluvial deposits because they can provide reasonably accurate quantitative estimates of paleoslope, an elusive yet important environmental variable.**

INTRODUCTION

Reconstructing depositional gradient from ancient deposits can be a powerful tool for determining surface dynamics of ancient landscapes. In net-aggradation systems and at basin-filling time scales, river gradient is set by water and sediment discharge (Whipple et al. 1998) and downstream sediment extraction due to deposition (Paola et al. 1992; Paola and Mohrig 1996; Whipple and Trayler 1996). Consequently quantitative paleoslope data from the stratigraphic record provide important insight into paleo-depositional conditions in basins, including information about climate, tectonics, and river dynamics. For example, paleoslope estimates enable comparisons between depositional slope and postdepositional tectonic movements (McMillan et al. 2002; Heller et al. 2003; Duller et al. 2012). Changes in fluvial profiles indicated by paleoslope measurements can also record changes in subsidence patterns (e.g., Paola and Mohrig 1996), sediment and water supply (Paola et al. 1992), or general landscape response to climatic and tectonic perturbations (Armitage et al. 2011). Paleoslope reconstructions may also be useful for identifying slope adjustments driven by autogenic reorganization of fluvial systems over relatively long timescales (Kim et al. 2006; Dalman and Weltje 2008). Furthermore, slope is an important morphodynamic measurement in rivers, which, if recoverable from ancient deposits and considered with other paleo-hydrophysiographic variables, may provide a means of quantitatively reconstructing paleodischarge from the sedimentary record—information that can be used both in paleoenvironmental analyses and in exploration and development of hydrocarbon reservoirs (Bhattacharya and Tye 2004).

Despite the potential value of paleoslope estimates, relatively few methods have been proposed for quantitatively reconstructing slope from ancient deposits. Several methods have been proposed for reconstructing other aspects of paleohydraulics in sandy fluvial systems. Bhattacharya and Tye (2004) and Bhattacharya and MacEachern (2009) extrapolated paleo flow velocities from published bedform phase diagrams (e.g., Rubin and McCulloch 1980) using grain size and channel geometries measured in ancient deposits. This information was then used to estimate paleodischarge and paleodrainage area; paleoslopes were derived from paleo flow velocity and flow depth. Although it is a reasonable attempt at a first-order estimate, this relationship may not be sufficiently accurate for many quantitative paleohydraulic reconstructions because the relationship between bedforms, grain size, and velocity is not as straightforward as portrayed in classical bedform phase diagrams (Jerolmack et al. 2006), and uncertainties associated with these estimates remain unconstrained.

Davidson and North (2009) proposed utilizing regional hydraulic-geometry curves to constrain paleocatchment size and paleodischarge from ancient deposits. They reconstructed paleodischarge from measurements of paleo flow depth and estimates of paleoclimate made in ancient deposits by using the relationship between drainage area and discharge established in modern systems with regional geomorphic and climatic characteristics similar to the ancient setting. These paleodischarge estimates, coupled with channel geometries measured in outcrop, provide a means to estimate average catchment-wide attributes, but they are untested for reconstructing spatial and temporal variations in paleoslope. They are suitable, however, as first-order approximations, useful in

Published Online: September 2014
 1527-1404/14/084-825/$03.00

combination with the methods proposed here, to better resolve the interpretation of the depositional environment.

Channel slope, discharge, depth, and width are key variables for understanding the dynamics of modern rivers. However, these variables are, at best, difficult to measure directly from ancient deposits. Paleoslope estimates, therefore, are best made using other data that can be obtained from fluvial deposits, including observations about particle size, shape, and sorting; bedform and barform heights and lengths; and often a measure of flow depth. Thus a useful paleoslope reconstruction strategy for sandy river deposits should include several key elements: 1) it must be based on river attributes measureable in ancient deposits, 2) it should produce relatively local measurements (reach-scale as opposed to drainage-scale or basin-wide averages), and 3) there must be some understanding, and preferably quantification, of uncertainties associated with the method. This last point is particularly important because validating paleohydraulic reconstructions of ancient deposits is nearly impossible and quantitative estimates of uncertainty are necessary to reliably interpret results.

Here we propose and test three methods, two empirical and one theoretical, for reconstructing paleoslope in sandy, suspended-load rivers that satisfy the above criteria. The first approach uses an empirical closure for sandy rivers that relates grain size of the bed-material load to flow depth and slope averaged over a channel reach. The second approach improves on the first by allowing the shear stress for incipient motion to vary with the dominant particle size. The third methodology builds upon a simple physical model that establishes depositional skin-friction shear stresses from assemblages of sedimentary structures and their associated grain-size distributions. Skin-friction shear stress plus a geometrically determined form-drag shear stress yields an estimate for the total boundary shear stress that is directly related to slope, averaged over an appropriate spatial scale. We test these methods with data from modern sand-bed rivers, where suspended load is dominant (median bed load particle diameter of very fine to medium sand, 0.0625–0.5 mm) and demonstrate that these approaches are capable of estimating the depositional gradient of a reach that is accurate to better than a factor of two. Ultimately, sedimentology and stratigraphy are inherently interpretive sciences, and any movement toward quantitative, physically based interpretation will serve to enhance our understanding of the deposition and preservation process.

PRELIMINARY CONSIDERATIONS

The methods presented below are based largely on established relationships derived from sediment transport studies in civil engineering. The relationships require assumptions to step from civil engineering—where hydraulic conditions can be directly measured in an active river reach—to sedimentary geology, where direct measurements of paleohydraulic and paleo-hydrophysiographic conditions are next to impossible. These methods use data from preserved alluvial river deposits, such as grain size and flow depth, and use the data to constrain the depositional conditions. These methods are applicable only to net aggradational systems with self-formed channels. In cases of significant erosion, such as incised valleys, these methods should only be applied to accurately reconstruct the valley-filling phase or phases.

Grain Size

This analysis focuses solely on sand-bed rivers whose dominant mode of sediment transport is suspension. Suspended-load rivers have a particle Reynolds number (Re_p) of $1.96 \leq \mathrm{Re}_p \leq 45.0$, as defined by Parker (2008) and Wilkerson and Parker (2011). Re_p is expressed as

$$\mathrm{Re}_p = \frac{D_{50b}\sqrt{(D_{50b}Rg)}}{v} \tag{1}$$

where D_{50b} is the median bed-material particle diameter, R represents the submerged specific gravity of the bed material ($R=(\rho_s/\rho)-1$), ρ_s is sediment density, ρ is water density, g is acceleration due to gravity, and v is the kinematic water viscosity. R is approximately 1.65 for quartz and $1.96 \leq \mathrm{Re}_p \leq 45.0$ corresponds to $0.062 \text{ mm} \leq D_{50b} \leq 0.50$ mm, or very fine to medium sand, using a constant value for v at 20°C.

Particle-size considerations are necessary because of the inverse correlation between Re_p and the nondimensional stress for incipient particle motion, or Shields number at bankfull flow ($\tau^*_{bf\,50} = H_{bf}S/RD_{50b}$, where H_{bf} is bankfull depth and S is bed slope, following Wilkerson and Parker 2011). This inverse relationship is shown clearly in Figure 1 for median bed-material particle diameters ranging from very fine sand to coarse pebbles, reproduced from the data used in Wilkerson and Parker (2011; their fig. 2). This relationship holds true for grain sizes beyond the studied range, and allowed Paola and Mohrig (1996) to devise a technique for estimating paleoslope in gravel-bed fluvial systems, where $D_{50b} \geq 2$ mm. Unfortunately, the Paola and Mohrig (1996) method cannot be directly applied to sand-bed systems, in part because drag resulting from bedforms is negligible in gravelly rivers dominated by lower plane beds. In contrast, drag from bedforms has significant influence on the relationship between bed shear stress and slope in sandy rivers (Parker 1978; Nelson and Smith 1989a, 1989b). The analyses here are thus limited to sand-bed rivers whose median grain diameter is very fine to medium sand ($0.0625 \leq D_{50b} \leq 0.5$ mm). It is beyond the scope of this paper to examine paleoslope reconstruction in coarse sand ($0.5 \leq D_{50b} \leq 2.0$ mm), mixed-load to bed-load dominant rivers.

Uncertainties

Reconstructed slopes are highly sensitive to the collected set of measured values. Primary sources of error are associated with natural-occurring variability that can be quantified by establishing careful data collection methods.

Flow Depth.—Flow depth, river depth, height, bankfull, reach-averaged, average, maximum, and cross-sectional-averaged are all sedimentological descriptors of river "depth," or H. Ancient river depth can be estimated from a variety of features, such as fully preserved barforms, dune cross-set thickness, dune heights, fining-upward sequences, and mud plugs (Paola and Borgman 1991; Leclair et al. 1997; Mohrig et al. 2000; Leclair and Bridge 2001; Leclair 2002; Leclair 2010).

All methods developed here take advantage of the general force balance for steady uniform flow, where

$$slope = \frac{total\ boundary\ shear\ stress}{fluid\ density \times gravitational\ acceleration \times flow\ depth}.$$

Flow depth is inversely proportional to slope, and small differences in flow depth may be the largest source of uncertainty for the proposed methods. This uncertainty can be managed, if not characterized, through careful outcrop measurements and the assembly of large datasets with statistically significant numbers of measurements. In fact, maximum river depths, found in scour zones, rarely exceed five times average flow depths in both experimental and modern rivers (Best and Ashworth 1997; Paola 1997). Local measures of flow depth seldom vary by more than an order of magnitude, and outcrop estimates of flow depth do not produce wide ranges in values (e.g., Mohrig et al. 2000; Foreman et al. 2012).

Grain Size.—We acknowledge the potential uncertainty associated with reducing a distribution of grain size to one characteristic value (Hajek et al. 2010), such as the median (D_{50}) or maximum percentile (D_{max}) particle diameter of a sample. Sampling uncertainties, natural spatial variability, and analysis errors are further complicated when working with the tail of

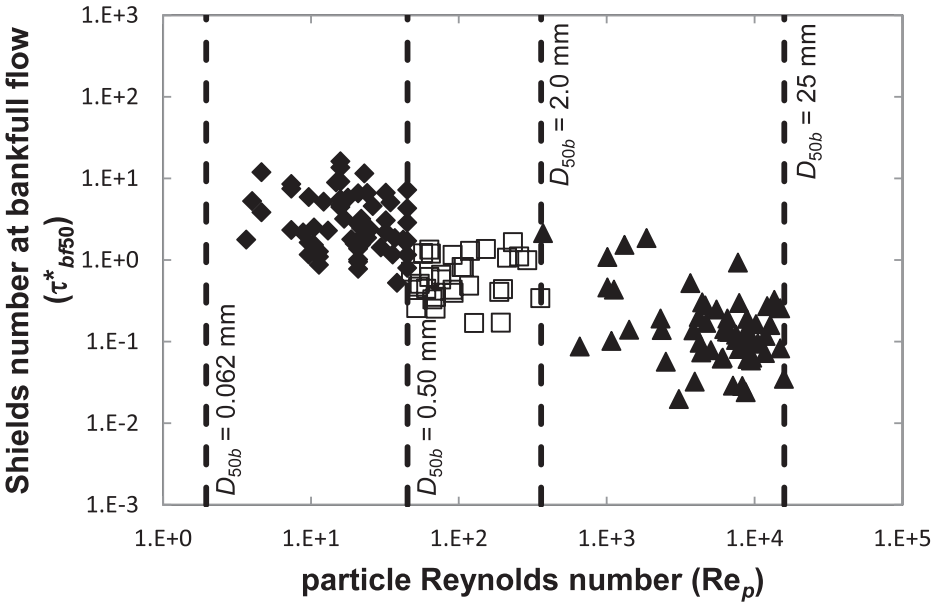

FIG. 1.—Shields number at bankfull flow plotted against the particle Reynolds number for $D_{50b} < 25$ mm. The solid diamonds represent 0.625 mm $< D_{50b} \leq 0.50$ mm, open squares are 0.50 mm $< D_{50b} \leq 2.0$ mm, and the solid triangles are 2.0 mm $< D_{50b} \leq 25$ mm. Data are from Wilkerson and Parker (2011). The inverse relationship between τ^*_{bf50} and Re_p holds over a large range of particle diameters.

a distribution and attempting to exclude outliers. For these reasons, we have chosen to use the 95th percentile of grain diameter, or D_{95}, to characterize D_{max}. This simplifying relationship is only used in the suspension criteria (third) method, and will have to suffice until entire grain-size distributions can be more fully incorporated into slope estimates.

Spatial and Temporal Constraints.—Excepting Holocene examples, detailed age control in preserved fluvial deposits is generally absent. Although relative constraints on timing of deposition can be determined using cut-and-fill relationships, interpretation of the three-dimensional spatial association of fluvial bedforms, barforms, and channels is consistently impeded by the lacking fourth dimension of time. It is nearly impossible to assert, even at the scale of a channel fill, that two series of bedforms are time-equivalent. It is even more difficult to associate those bedforms with time-equivalent slackwater deposits and flow depths. The paleo-fluvial record forces the amalgamation of space and time, and all paleohydraulic estimators fall under these constraints.

Data

The paleoslope reconstruction methods were tested for consistency using modern sand-bed rivers. Modern rivers allow for unambiguous measurements of flow depth, bed-material load, suspended load, and slackwater deposits, which can be used as a proxy for suspended load (Lynds and Hajek 2006; Hajek et al. 2010). Modern rivers have the added advantage of measureable *in situ*, reach-averaged slopes that can be used to validate the reliability of calculated slopes.

Three different datasets were employed in this study. Wilkerson and Parker (2011) data were compiled from numerous sources (their table 1). For this analysis, their data were reduced to 60 individual rivers or river reaches with median bed grain diameters less than 25 mm to demonstrate the inverse correlation between the particle Reynolds number and Shields number at bankfull flow that holds for a large range of grain sizes (Fig. 1). Twenty-five of these river or river reaches have median bed grain diameters that range from very fine to medium sand.

The second dataset was compiled by Brownlie (1981). This large dataset has a total of 1202 measurements of slope, median bed-material grain diameter, and flow depth, including 107 measurements of very fine sand (0.0625 mm $\leq D_{50b} \leq$ 0.125 mm), 452 of fine sand (0.125 mm $\leq D_{50b} \leq$ 0.250 mm), and 643 of medium sand (0.250 mm $\leq D_{50b} \leq$ 0.50 mm).

The third dataset includes samples collected by the authors (summarized in Lynds 2005). The data, in addition to sample collection and processing methods, are available as Supplemental Material. This dataset includes measurements of particle diameter and flow depth from the North Loup, Niobrara, and Calamus rivers in Nebraska, U.S.A. (Fig. 2). The data contain 28 sediment measurements from active dune crests, 40 suspended-load samples, and 25 slackwater deposits, in addition to flow-depth measurements from each sample location as well as 18 cross-stream profiles of channel topography. These additional data are important because the Wilkerson and Parker and the Brownlie datasets summarize only D_{50b}. The Lynds data contain grain-size distributions from suspended-load and slackwater samples, which are essential for the analysis of the suspension criteria (third) method.

Error Analysis

Each method is tested against the available datasets to determine how well the estimated slope compares to the measured slope of modern rivers with known parameters. All results are shown on log-log plots of estimated and measured slope. Fit is assessed by percentage estimation error, $100(e - m)/m$, where e and m are the estimated and measured slopes, respectively. Positive values of the percentage estimation error denote overestimation, negative values denote underestimation. The root-mean-square (RMS) error is also reported when applicable. RMS error aggregates the residual differences between e and m into a single measure with units of, in this case, slope. RMS error $= \sqrt{\left(\sum (e-m)^2\right)/n}$, where n is the number of observations.

METHOD 1: CONSTANT SHIELDS NUMBER AT BANKFULL FLOW

Strategy

Easily obtained field discriminators, including the composition of the active channel bed, or bed-material load, and the bankfull flow depth, are

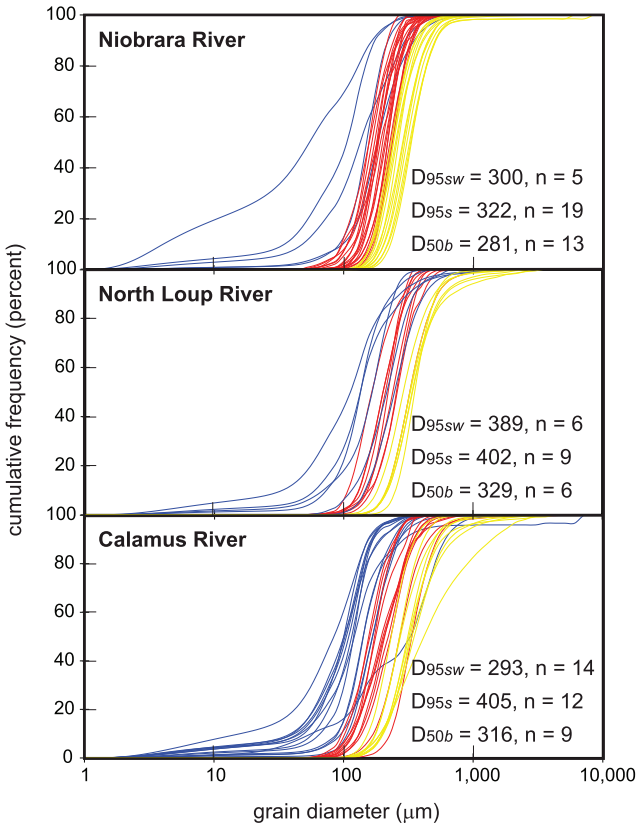

FIG. 2.—Cumulative frequency plots of grain diameter from three sand-bed rivers in Nebraska. Blue lines represent slackwater samples, red are samples of active suspended load, and yellow are active bed-material load. D_{95sw} is the mean 95th percentile grain diameter of slackwater samples, D_{95s} is the mean 95th percentile grain diameter of suspended load samples, and D_{50b} is the mean 50th percentile grain diameter of bed-material load samples. All sample diameters are in microns (μm), n denotes the number of samples for each sample type.

combined for a first-order estimate of river slope, based on Parker's (1978) general relation for channel form:

$$\frac{H}{D}S = R\tau_a^*, \tag{2}$$

where H is flow depth, D is a particle diameter, S is water-surface slope, and τ_a^* is a nondimensional bankfull shear stress. Following this general form, the reach-averaged water-surface slope is a function of bed material, particle diameter, river depth, and τ_a^*. Equation 2 can be used to estimate slope by substituting the bankfull flow depth (H_{bf}) for H (see Preliminary Considerations on flow depth), the median bed-material grain diameter (D_{50b}) for D (intended as an average snapshot of the bed material transported by the river system; see Preliminary Considerations on grain size), and the Shields number at bankfull flow (τ_{bf50}^*) for τ_a^*, yielding

$$S = \frac{\tau_{bf50}^* R D_{50b}}{H_{bf}}. \tag{3}$$

When working with ancient fluvial systems, H_{bf} is measurable from the outcrop, and D_{50b}, although possibly not well-constrained in the field from a visual estimate, can be accurately determined using simple laboratory techniques. Therefore, τ_{bf50}^* is typically the only unknown on the right-hand side of Equation 3. Figure 3 shows a plot of τ_{bf50}^* against bankfull flow depth using the Wilkerson and Parker dataset for $0.062 \text{ mm} \le D_{50b} \le 0.50$ mm. These suspended-load rivers encompass a range of flow depths from less than one meter to greater than 10 meters, while maintaining an average value for τ_{bf50}^* that varies only over one order of magnitude. This method thus estimates slope for suspended-load rivers (Equation 3) by assuming a constant value for τ_{bf50}^*, determining the median grain diameter and composition of the bed material, and measuring the bankfull flow depth. The errors associated with slope estimation for suspended-load rivers are minimized when $\tau_{bf50}^* = 1$ which is the near-minimum value observed from the Wilkerson and Parker dataset (Fig. 3).

Application

Following Equation 3, estimated slopes are plotted against measured slopes for the Brownlie dataset (Fig. 4). The consistent estimation trend for river slopes varies over three orders of magnitude. The median estimation error for very fine sand ($0.062 \text{ mm} \le D_{50b} \le 0.125$ mm) is -9.0 percent, with an RMS error of 5.16×10^{-5}. Fine sand ($0.125 \text{ mm} < D_{50b} \le 0.250$ mm) has a median estimation error of -14.5 percent, with an RMS error of 1.48×10^{-3}. Medium sand ($0.250 \text{ mm} < D_{50b} \le 0.500$ mm) yields a median estimation error of +8.4 percent, and an RMS error of 1.61×10^{-3}. The median estimation error for all samples, not subdivided by grain diameter, is -2.2 percent with an RMS error of 1.49×10^{-3}.

Discussion

A quick and simple assessment of depositional slope is a powerful field tool. Flow depth can be easily measured in the field; however, D_{50b} is always most accurately determined by processing numerous samples for grain size in the laboratory.

It is necessary to stress that the disadvantage to this method is that it will never yield more than a rough estimate of depositional gradient; the benefit is in its simplicity and ease of application. For example, field-derived results could be useful in a teaching program on fluvial depositional systems, or used to guide a researcher to specific localities or outcrops that may contain key information for a regional interpretation. It is our hope that this method will be used as a simple first approximation of river slope, but not as a tool for in-depth analyses of ancient fluvial systems.

Summary

With the assumptions that $\tau_{bf50}^* = 1$ and $R = 1.65$ for quartz, data required for this method include only an estimate of D_{50b} and H_{bf}. Equation 3 reduces to

$$S = \frac{1.65 D_{50b}}{H_{bf}}. \tag{4}$$

METHOD 2: VARYING SHIELDS NUMBER AT BANKFULL FLOW WITH GRAIN SIZE

Strategy

The constant Shields number at bankfull flow method outlined above does not account for its known variation as a function of the Reynolds particle number, a proxy for grain size (Fig. 1). This second method provides a more physically justified and accurate approach that accounts for this inverse relationship.

Allowing Shields number at bankfull flow to vary with grain size leads to a paleoslope calculation method that hinges on the ratio of skin-friction shear velocity (u_{sf}^*) to particle settling velocity (w_s) or u_{sf}^*/w_s. If the settling velocity for a specific grain size is much greater than the shear velocity predicted to

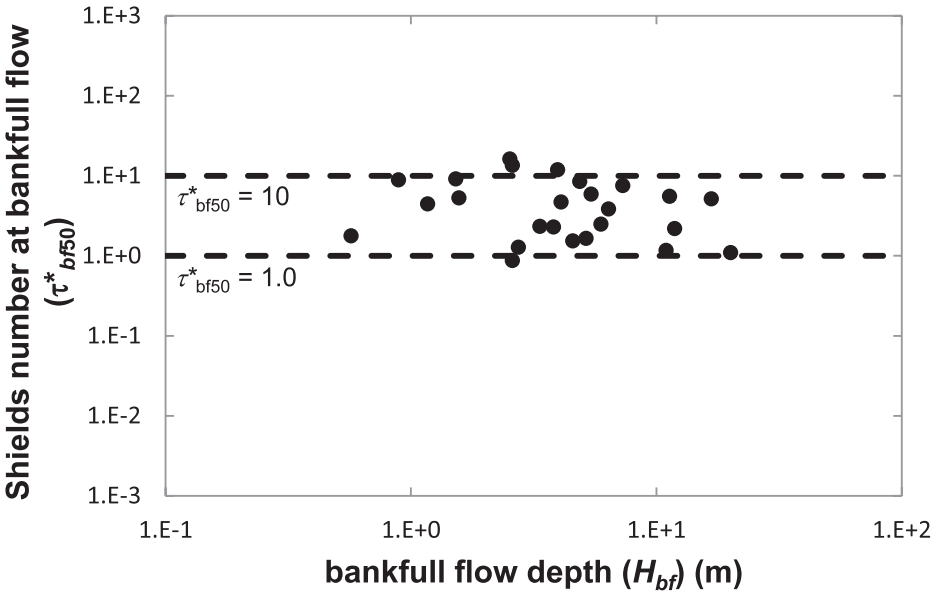

FIG. 3.—Shields number at bankfull flow plotted against bankfull flow depth for the Wilkerson and Parker (2011) dataset, for 0.625 mm $< D_{50b} \leq$ 0.50 mm. H_{bf} varies over more than an order of magnitude, and τ^*_{bf50} ranges from approximately 1.0 to 10.0.

keep it in suspension, the particle will be transported as bed load, if it moves at all. Conversely, if w_s is of the same order as u^*_{sf}, the given particle size will be carried in suspension. As mentioned previously, this study focuses specifically on rivers with suspension as the dominant mode of sediment transport.

The change from pure bed-load transport to full suspension transport is gradational, yet experimental work has helped define criteria for bed-load to suspended-load transport conditions. Experimental studies by Laursen (1958) and Niño et al. (2003) independently established the same minimum threshold for incipient suspension, of $u^*_{sf}/w_s = 0.4$. The sediment-flux data assembled in Laursen (1958) defined this threshold for suspension by the first departure in the trend for bed-load flux as a function of bed stress. Niño et al. (2003) directly observed the near-bed layer of sediment transport and defined the suspension threshold by the first observed grains being advected into the interior of the flow by turbulent eddies. Data from Laursen (1958) can also be used to define the transition from suspension to washload at $u^*_{sf}/w_s \geq 3.0$ (Smith and Hopkins 1972). Julien (2010) determined that bed load is dominant for $0.2 < u^*_{sf}/w_s < 0.5$, mixed-load transport occurs for $0.5 < u^*_{sf}/w_s$

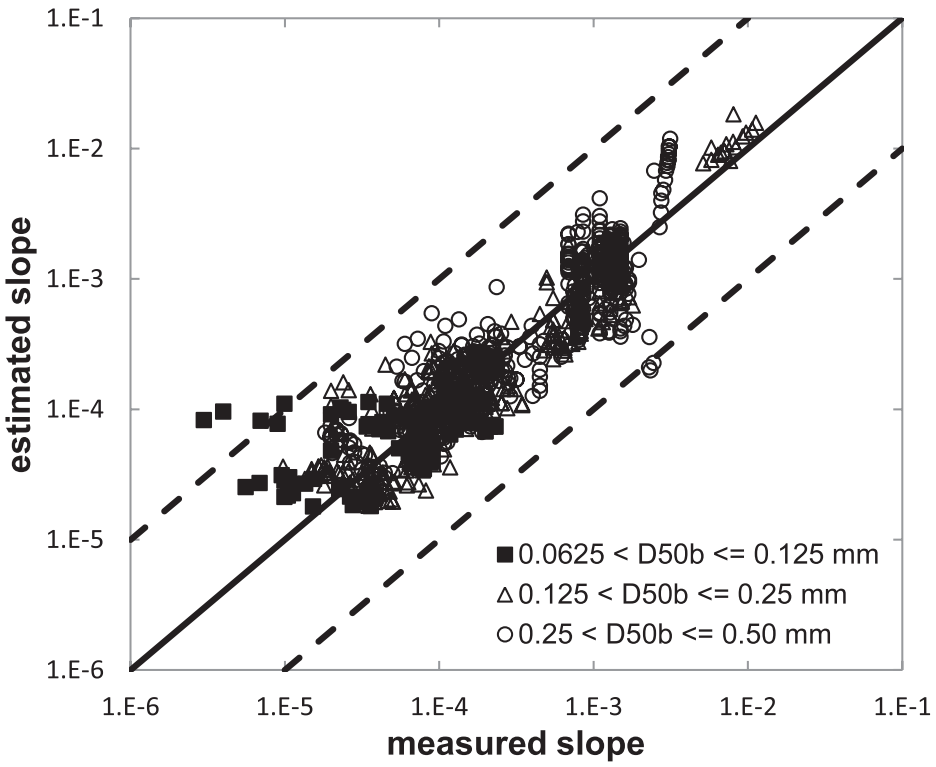

FIG. 4.—Estimated slope plotted against measured slope for the Brownlie (1981) dataset using the constant Shields number at bankfull flow method (method 1). The solid diagonal line shows perfect slope estimation; the dashed lines are overestimation and underestimation by an order of magnitude.

< 2.0, and suspended-load transport is prevalent for u^*_{sf}/w_s greater than 2.0. The question then becomes: what is an appropriate single metric for suspension that can be drawn from this range?

Wilkerson and Parker (2011) show that for suspended-load rivers

$$\frac{u^*_{sf}}{w_s} = \frac{\sqrt{\tau^*_{bf50}}}{\left(W_*/Re_p\right)^{1/3}}. \tag{5}$$

There are numerous approaches in the literature to determine w_s for a given grain size (e.g., Riley and Bryant 1979; Dietrich 1982; Jimenez and Madsen 2003; Ferguson and Church 2004). The approach chosen may depend on particle shape, potential flow conditions, and individual preference or familiarity. We employ the approach defined by Dietrich (1982), where the dimensionless settling velocity (W^*) is

$$\begin{aligned}\log W^* = &-3.76715 + 192944(\log D^*) - 0.09815(\log D^*)^2 \\ &- 0.00575(\log D^*)^3 + 0.00056(\log D^*)^4\end{aligned} \tag{6}$$

and the dimensionless particle size (D^*) can be described as a function of the grain density (ρ_s) and fluid density (ρ), the particle diameter (D), and kinematic fluid viscosity (v):

$$D^* = \frac{(\rho_s - \rho)gD^3}{\rho v^2}, \tag{7}$$

for $0.22 \leq \mathrm{Re}_p \leq 7.1 \times 10^4$ (different equations are used for Re_p values outside of the designated range; see Dietrich 1982, for complete discussion). Finally, the settling velocity can be calculated as

$$w_s = \left[\frac{W^*(\rho_s - \rho)gv}{\rho}\right]^{1/3}. \tag{8}$$

Solving Equations 3 and 5 for the Shields number at bankfull flow yields

$$\left(\frac{u^*_{sf}}{w_s}\left(W_*/Re_p\right)^{1/3}\right)^2 = \tau^*_{bf50} = \frac{H_{bf}S}{RD_{50b}}. \tag{9}$$

Equation 9 is rearranged to solve for slope:

$$S = \frac{RD_{50b}}{H_{bf}}\left(\frac{u^*_{sf}}{w_s}\left(W_*/Re_p\right)^{1/3}\right)^2. \tag{10}$$

All variables in this equation are measurements that can be obtained from the system being studied, specifically bankfull flow depth and grain size.

Application

Following Julien's (2010) assessment, it is reasonable to set u^*_{sf}/w_s equal to 2.0, the value at which suspended load becomes dominant. Estimated versus measured slope is plotted in Figure 5A for $u^*_{sf}/w_s = 2.0$, using the Brownlie dataset. For nearly every case, the measured slope is estimated within an order of magnitude, with a median estimation error of -8.1 percent and an RMS error of 1.69×10^{-3}.

However, the estimation error can be reduced if u^*_{sf}/w_s is modified for grain size. When D_{50b} values in the range of medium sand ($0.25 \leq D_{50b} \leq 0.50$ mm) are isolated, the median estimation error for slope is reduced to -0.75 percent (RMS error of 1.18×10^{-3}) for $u^*_{sf}/w_s = 1.6$ (Fig. 5B), suggesting that mixed load is dominant for rivers with beds composed of medium sand. The error can also be reduced for fine and very fine sand ($0.0625 \leq D_{50b} \leq 0.25$ mm) using $u^*_{sf}/w_s = 3.1$ (Fig. 5B). For this case, the median estimation error is reduced to +0.93 percent with an RMS error of 1.99×10^{-3}. Presumably rivers with beds primarily composed of very fine to fine sand are transporting all grain sizes in full suspension under conditions that are consistent with Laursen's (1958) definition for full suspension of $u^*_{sf}/w_s \geq 3.0$.

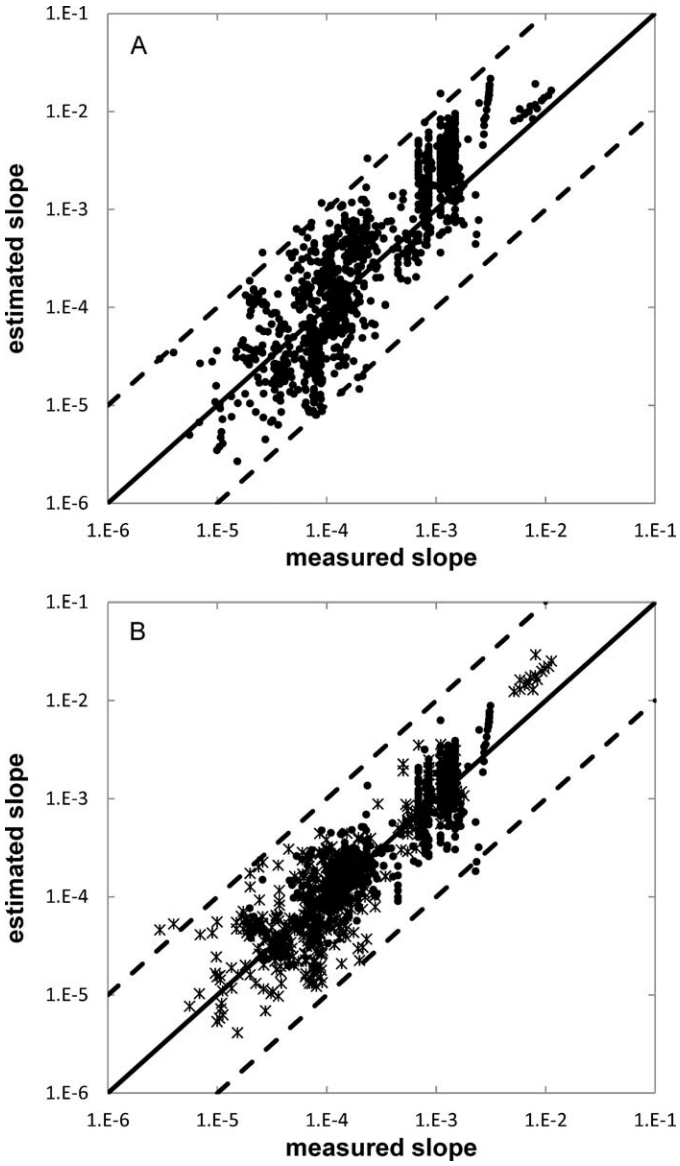

FIG. 5.—Estimated slope plotted against measured slope for the Brownlie (1981) dataset using the varying Shields number at bankfull flow method (method 2). The solid diagonal line shows perfect estimation; the dashed lines are overestimation and underestimation by an order of magnitude. **A)** $u^*_{sf}/w_s = 2.0$. **B)** u^*_{sf}/w_s is optimized for grain size, where $u^*_{sf}/w_s = 3.1$ for $0.625 \text{ mm} < D_{50b} \leq 0.25$ mm (asterisks) and $u^*_{sf}/w_s = 1.6$ for $0.25 \text{ mm} < D_{50b} \leq 0.50$ mm (solid circles).

Discussion

Accounting for the decrease in Shields number at bankfull flow with increasing particle diameter is preferred to assuming a constant Shields number at bankfull flow. As expected, this second method significantly reduces the estimation error compared to the first method, producing a more reasonable estimate of river gradient.

The results presented in Figures 5A and 5B highlight the advantage of a very large dataset. Any single slope calculation could be incorrect by up

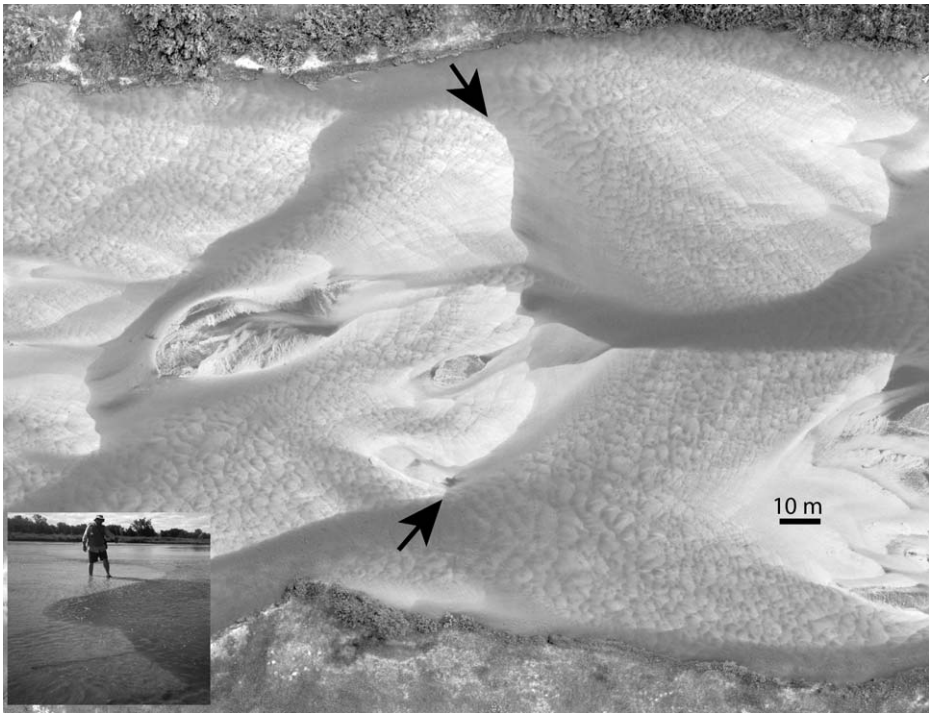

FIG. 6.—Aerial photo of North Loup River near Taylor, Nebraska. Flow is from left to right. The two arrows mark the cross-stream extent of a mid-channel compound bar. The smooth river-bottom surfaces in the lee of this bar are constructed of grain-fall (suspension) deposits that accumulate in this slackwater. Inset) Person standing at the crest of a mid-channel bar in the North Loup River. Notice that the barform nearly reaches the water surface, producing the slackwater zone immediately downstream of the bar.

to an order of magnitude. It is only in the aggregate that the estimated slope agrees with the measured slope, and in fact varies by a factor no more than 1.3. The problem then becomes one of data volume. To the authors' knowledge, a dataset as large as Brownlie's (1981) has yet to be assembled for any single rock formation. A typical dataset from the rock record might include several tens of grain-size determinations and measurements of flow depth. The error associated with calculating paleoslope at a specific location, using local measurements of paleo flow-depth and particle diameter of the bed-material load, will thus be in the range of better than a factor of two. Although a factor of two may be an acceptable approximation, the third paleoslope method is preferable because it yields the most accurate estimates using small datasets that are most commonly collected from outcrops of fluvial deposits.

Summary

The most promising application of this second method follows these steps:

1. Accurately determine D_{50b} through laboratory analyses of collected sediment samples and H_{bf} from field measurements.
2. $R = 1.65$ for quartz, or should be determined independently if quartz is not the primary composition of the sediment.
3. Establish W_* using Equations 6 and 7.
4. Calculate Re_p using Equation 1.
5. Subdivide samples into two categories: very fine to fine sand ($0.0625 \leq D_{50b} \leq 0.25$ mm) and medium sand ($0.25 \leq D_{50b} \leq 0.50$ mm).
6. Solve for slope (Equation 9) using $u^*_{sf}/w_s = 3.1$ for D_{50b} values representing very fine to fine sand and $u^*_{sf}/w_s = 1.6$ for medium sand.

METHOD 3: SUSPENSION CRITERIA

Strategy

The constant and varying Shields number at bankfull flow methods benefit from simple measurements and application of only one primary equation. This final approach determines channel slope by a more comprehensive evaluation of sediment transport in sandy suspended-load rivers. Although this method is more complicated, its benefit is improved accuracy of paleoslope estimations because each structure in an active channel (and preserved in the rock record) is connected to the suite of other structures in a way that is consistent with the flow and sediment-transport mechanics of the system. For example, estimates of channel depth from preserved sets of dunes must agree with estimates from preserved barforms, and particle sizes interpreted as transported in the suspended load must be consistent with the grain sizes carried in the active layer along the channel bed. That is, particle sizes representing two different but simultaneously occurring modes of sediment transport (suspended load and bed-material load) must be connected to a single flow field (Fig. 2).

This method determines slope by reconstructing flow and sediment-transporting conditions in sand-bed rivers by taking advantage of all available physical sedimentary structures and textures preserved in their deposits. The approach focuses on using grain-size distributions of suspended sediment to reconstruct the component of the total boundary shear stress specifically associated with sediment transport, the skin-friction shear stress (Nelson and Smith 1989a). Sediment deposited solely from suspension can be found in zones of slackwater, often located in the lee of bar forms (Fig. 6). These sites of suspended-sediment deposition and resulting slackwater deposits in both modern and ancient examples have been previously described by Lynds and Hajek (2006) and Hajek et al. (2010). To generate accurate estimates of longitudinal slope of the river system, the values of the skin-friction shear stress are transformed into values of total boundary shear stress by adapting the methods of Smith and McLean (1977) and Nelson and Smith (1989a) for quantifying the form drag associated with topographic elements of a channel, as described below.

Components of the Total Boundary Shear Stress.—For steady uniform flow, the force balance defining the total boundary shear stress (τ_b) is

$$\tau_b = \rho g H S \tag{11}$$

where ρ is fluid density, g is gravitational acceleration, H is spatially averaged flow depth, and S is spatially averaged water-surface slope. This

FIG. 7.—Outcrop photograph showing dune-scale cross stratification (dipping toward the left) within larger bar-scale cross stratification (dipping toward the right). White field notebook is approximately 12 cm tall. Photograph from the Jurassic Kayenta Formation, Colorado National Monument, Colorado.

relationship between the flow and its container can be applied to all natural channels with some error. Related error is minimized when values for H and S are averaged over an appropriate channel section (Nelson and Smith 1989a). Spatial averaging incorporates all bed and bank irregularities into the effective roughness of the channel and contributes to τ_b as a form drag, or momentum deficit, arising from adverse pressure distributions on the irregular channel topography. The sum of the form drag and skin friction is τ_b and is thus given by

$$\tau_b = \tau_{sf} + \tau_{fd}, \tag{12}$$

where τ_{sf} is the skin-friction shear stress that is directly responsible for sediment transport and τ_{fd} is the form drag boundary shear stress associated with bed and bank irregularities.

Reconstructing τ_{sf} from Deposits.—Each particle transported by a river has two intrinsic properties relating it to the flow field: 1) the critical shear stress for initial motion of that clast size (τ_{cr}), and 2) a settling velocity (w_s) that acts to remove the particle from suspension (Bagnold 1966). In gravelly systems, τ_{sf} for the bankfull channelized flow and τ_{cr} for the bed material are approximately equal in value and the critical shear stress is the appropriate grain parameter to use in paleohydraulic reconstructions (Paola and Mohrig 1996). In sandy systems, τ_{sf} for the flow can be many times greater than τ_{cr} for the bed material. There is no unique relationship between τ_{sf} and τ_{cr} for sand bed rivers; therefore a different transport criterion must be established.

If a characteristic value exists for the ratio of skin-friction shear velocity to particle settling velocity, or u^*_{sf}/w_s, then τ_{sf} can be estimated with the calculation of the particle settling velocity using the established relationship $u^*_{sf} = \sqrt{\tau_{sf}/\rho}$ (Wilkerson and Parker 2011). Unlike in the second method, where we were interested in empirically relating u^*_{sf}/w_s to significant transport in suspension, we are interested instead in determining a value for the onset of a measurable suspended-sediment concentration profile, best defined from the coarsest particles transported in suspension. For this threshold we have chosen to employ the Bagnold (1966) criterion for suspension transport of $u^*_{sf}/w_s = 1.0$. This value falls between the previously mentioned values for threshold and saturated suspended sediment transport.

To test the validity of the Bagnold criterion, u^*_{sf}/w_s was calculated from the coarsest representative particles (D_{99s}) of 34 suspended sediment samples collected from the North Loup River (flow depth less than 0.6 m; Mohrig 1994; Mohrig and Smith 1996). u^*_{sf}/w_s ranged from 0.56 to 1.27 (mean 0.77)—close to, but slightly less than, the Bagnold criterion—approaching agreement with the measurements of Niño et al. (2003) where $u^*_{sf}/w_s = 0.4$. The approximate validity of the Bagnold criterion as applied to D_{99s} of the suspended load holds for channels much deeper than the North Loup River. Measurements collected during floods of the Colorado River (flow depth of 7 m; Topping et al. 1999) and Waal River (flow depth of 10 m; Kleinhans et al. 2007; Frings and Kleinhans 2008) produce mean ratio values of 1.67 and 1.3, respectively. For the purpose of estimating τ_{sf} from the D_{99s} of the suspended load, the Bagnold criterion ($u^*_{sf}/w_s = 1.0$) appears to be a reasonable approximation, although future research could further refine this value.

This method relies on characterizing the suspension threshold, or the maximum particle size transported in suspension. This particle diameter can be difficult to classify due to uncertainties in spatial averaging as well as using the tail of a distribution. For these reasons, the general term D_{maxs} is used to represent the maximum particle diameter suspended within the flow at a measurable quantity.

Reconstructing τ_{fd} for Sandy Channels.—An analysis by Nelson and Smith (1989a) indicates that about 90 percent of form drag is caused by dunes in rivers where the bedforms grow to an average height and length that is limited by the depth of flow (e.g., Yalin 1977; Allen 1982; Nelson and Smith 1989b). The slope calculations developed here assume that the bed of the river is mantled by depth-limited dunes. The validity of this assumption to any particular sandy fluvial system can be confirmed by observing the presence of dune and bar deposits preserved in channel fills, thus establishing that barforms are composed primarily of dunes (for example, Fig. 7).

The Nelson and Smith (1989a) expression for the form drag associated with a train of dunes (τ_d) is

$$\tau_d = \tau_{sf} \frac{C_d}{2k^2} \frac{h_d}{\lambda} \left[\ln \left[\frac{h_d}{(z_o)_{sf}} \right] - 1 \right]^2 \tag{13}$$

where C_d is an empirically determined drag coefficient, equal to 0.21 for separated flow (Smith and McLean 1977; Nelson et al. 1993), k is von Kármán's constant (0.407), h_d is mean dune height, λ is mean dune length, and $(z_o)_{sf}$ is the bed roughness produced by saltating sediment. Equation 13 shows why depth-limited dunes, when present, are the major contributor to the form drag in a channel. Compared to other bedforms, depth-limited dunes are relatively steep (h_d/λ) and relatively tall (h_d); bars are somewhat taller, forming larger barriers to the flow, but are not nearly as steep as dunes, while ripples have a steepness similar to that of dunes but are not nearly as tall. As a result, for rivers mantled with depth-limited dunes, we employ the simplifying relationship $\tau_{fd} = \tau_d$.

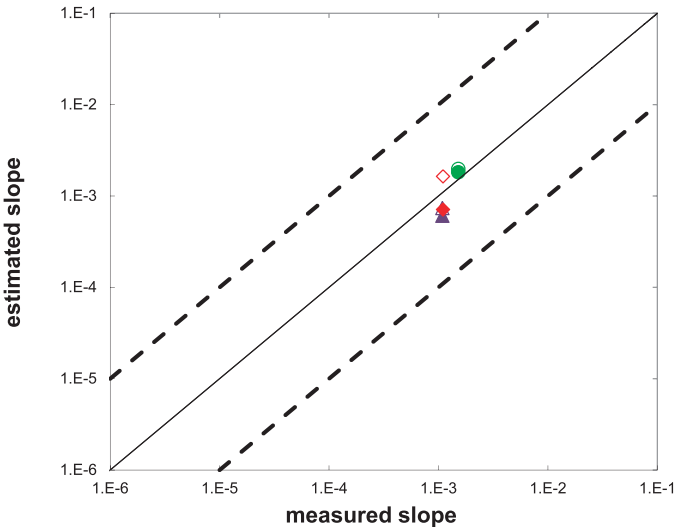

FIG. 8.—Measured versus estimated slope for the Niobrara (purple triangles), North Loup (green circles), and Calamus (red diamonds) rivers. The closed shapes represent calculations from slackwater deposits, and the open shapes are active suspended-load samples. Calculations were made using the average maximum flow depth, mean D_{95s}, and mean D_{50b}. The results are summarized in Table 1. The solid diagonal line shows perfect estimation; the dashed lines are overestimation and underestimation by an order of magnitude.

Combining Equations 12 and 13 yields the following expression for the ratio of total boundary shear stress to skin-friction shear stress (F):

$$F = \frac{\tau_b}{\tau_{sf}} = 1 + \frac{C_d}{2k^2}\frac{h_d}{\lambda}\left[\ln\left[\frac{h_d}{(z_o)_{sf}}\right] - 1\right]^2. \quad (14)$$

Theoretical discussion and analysis of Guy et al.'s (1966) laboratory data by Wiberg and Rubin (1989) show that $(z_o)_{sf}$ can be described as a function of the average saltation height, or the bed-load layer height, b. Wiberg and Rubin (1989) demonstrate that for a range of six different transport stages, the average $(z_o)_{sf} = 0.056b$ is valid within 95 percent confidence limits. We recognize that the height of the bed-load layer is not constant and varies with shear stress. However, to simplify to a value that can be estimated from the rock record and because Equation 14 depends only weakly on $(z_o)_{sf}$, we propose using Nelson and Smith's (1989a) approximate relationship $b \approx 2.0D_{50b}$.

The mean height and length of depth-limited dunes are estimated here using the maximum values from the theoretical analysis of Fredsøe (1982), where h_d is equal to $0.30H$ and the dune height-to-length ratio (h_d/λ) is 0.063, as validated by Yalin's (1992) data compilation. The mean dune height and steepness values described by Fredsøe (1982) are similar to the empirical values found in the Calamus River (mean steepness of 0.052; Gabel 1993) and North Loup River (mean steepness of 0.061 and 0.049, for flow depths of 0.5 and 0.2 m, respectively; Mohrig 1994).

Reconstructing River Slope.—A minimum suspension criterion of $u^*_{sf}/w_s = 1.0$ (Bagnold 1966) gives a value for u^*_{sf} equal to the settling velocity of the diameter of the coarsest grain (D_{maxs}) in suspension ($w_{s(Dmaxs)}$). Following $u^*_{sf} = \sqrt{\tau_{sf}/\rho}$,

$$\tau_{sf} = \rho\left(w_{s(Dmaxs)}\right)^2. \quad (15)$$

From Equations 14 and 15, the total boundary shear stress is related to τ_{sf} by Equation 12:

TABLE 1.—*Estimation error of the measured reach-averaged slope using the suspension criteria method for both suspended load and slackwater deposits. Estimation error represents the average value of each sample type for each river.*

River	Sample Type	Estimation Error (%)	Number of Samples
Niobrara	Suspended load	−32.0	19
	Slackwater	−44.0	5
North Loup	Suspended load	30.7	9
	Slackwater	20.1	6
Calamus	Suspended load	49.1	12
	Slackwater	−34.4	14

$$\tau_b = F\rho\left(w_{s(Dmaxs)}\right)^2. \quad (16)$$

Combining Equation 16 with Equation 11 gives the following equation required for estimating paleoslopes (S):

$$S = \frac{F\left(w_{s(Dmaxs)}\right)^2}{g\langle H\rangle}. \quad (17)$$

This suspension method, Equation 17, takes advantage of collectable outcrop data (D_{50b}, D_{maxs}, and H) and predicts depositional gradient with a reasonable degree of confidence, as demonstrated below.

Application

The suspension method (i.e., Equation 17) was tested on the Lynds dataset (Supplemental Material) which includes full bed-material and suspended-load particle size distributions. Equation 17 is solved by combining the spatially averaged flow depth (H, in this case the average maximum thalweg depth from two to ten flow-perpendicular transects of each river; see discussion below) with measured grain diameters. D_{50b} was obtained from active dune crests. D_{95s} was sampled from both the active suspended load and slackwater deposits, which are presumed to record the suspended load, and is used as a proxy for D_{maxs} (see Preliminary Considerations on grain size).

Figure 8 plots estimated slope against measured slope, with percentage estimation errors summarized in Table 1. Estimation errors range from −44.0 percent to +49.1 percent.

Discussion

Although the suspension method is the most involved, Equation 17 still has only three unknown variables: H, D_{50b}, and D_{95s}. Determinations of grain diameter are thus limited by accurate interpretation of the appropriate sedimentary structures and granulometry procedures—two manageable limitations. H, however, can be assessed in any number of ways on an active river. The average flow depth across a given reach is always significantly less than the maximum channel-thread thalweg depth, which accounts for less than 15 to 20 percent of the bed area in the studied rivers. Even so, the most suitable measure of flow depth should be thalweg depth because it most closely represents measures of flow depths from preserved sedimentary strata. The results for this method use the average maximum flow depth calculated from numerous cross-stream transects (six, two, and ten transects on the North Loup, Niobrara, and Calamus rivers, respectively; Supplemental Material).

The uncertainties associated with measurements of grain size and flow depth, as well as the assumption of uniform flow that allows use of the simplified force balance, highlight the importance of spatial averaging. Two tests were made to enumerate the uncertainty associated

TABLE 2.—*Estimation and RMS error of the measured reach-averaged slope using the suspension criteria method, for both suspended load and slackwater deposits, for individual samples with their associated* in situ *water depth. Estimation error represents the average value of each sample type for each river.*

River	Sample Type	Estimation Error (%)	RMS Error	Number of Samples
Niobrara	Suspended load	209.7	2.7×10^{-3}	8
	Slackwater	111.7	2.6×10^{-3}	5
North Loup	Suspended load	613.2	1.1×10^{-2}	8
	Slackwater	216.2	4.6×10^{-3}	6
Calamus	Suspended load	152.1	1.9×10^{-3}	6
	Slackwater	263.1	9.2×10^{-3}	12

with spatial averaging. First, river slope was estimated from Equation 17 for each individual suspended sediment and slackwater deposit and their local, *in situ*, flow depth. The results, averaged for each case and summarized in Table 2, show estimation errors as large as 613.2 percent.

For the second test, slope was determined using local values for D_{95s} of the suspended material and slackwater sediment (as in the previous case), with the measured reach-average maximum flow depth calculated from several cross-stream transects. The resultant slope estimations for each case were averaged as before and are reported in Table 3. Estimation errors are much less than for those determined using individual D_{95s} and H (Table 2) but are generally slightly higher than for reach-integrated grain-size values (Table 1). These encouraging results demonstrate that spatial averaging of $D_{\max s}$ and H over at least one channel reach sufficiently improves slope estimation, an important yet necessary step when working with outcrop samples.

Summary

Implementation of the suspension method can be subdivided into five steps.

1. Collect outcrop information and samples. Data collected at the outcrop should include spatially averaged flow depth H and samples representative of bed-material load and suspended load. Best candidates for bed-material load samples include dune- and bar-scale cross-stratification. Suspended-load samples should be from slackwater deposits.
2. Determine D_{50b} from the bed-material load samples and D_{95s} from the suspended-load samples in the laboratory. Many methods can be used for these analyses, including sieving, but a method that can accurately determine particle dimensions at the micron scale is preferable.
3. Resolve the ratio of the total boundary shear stress to skin-friction shear stress (F), using Equation 14 and the following assumptions explained previously: $C_d = 0.21$; $k = 0.407$; $h_d = 0.30H$; $h_d/\lambda = 0.063$; and $(z_o)_{sf} = 0.056(2D_{50b}) = 0.112D_{50b}$.
4. Determine the settling velocity of the coarsest suspended-load grain diameter, ($w_{s(Dmaxs)}$), where $D_{maxs} = D_{95s} \cdot w_{s(D_{95s})}$ is solved with Equations 6, 7, and 8.
5. Solve Equation 17 for paleoslope.

CONCLUSIONS

The application of these methods has been demonstrated using modern sand-bed rivers with suspension as the primary mode of sediment transport. The foundation has been set for the direct application of these approaches to the ancient fluvial rock record. The primary implications from this study are:

1. Combined analysis of data from modern sandy rivers and assessment of errors associated with estimates of sediment transport and paleodepth indicate that the paleoslopes associated with sandy channel fills can be estimated to less than a factor of two.
2. The first two methods are based upon empirical observation and require only an estimate of the median bed-material grain diameter, which can be unambiguously observed and sampled in the field or in core. The third method, although more reliable and physics-based, depends on samples of suspended sediment, which can be ambiguous to interpret and difficult to disaggregate for grain-size determination. For now, and until future work defines the limits of these methods in the sedimentary rock record, paleoslope estimates should aim to use a combination of these methods, whenever possible, yet focus on the final suspension method.
3. Using approaches such as these enables the reconstruction of depositional profiles from reach-averaged data. It is possible to go beyond a basin-averaged snapshot and piece together slope differences across a basin and through time.
4. The methodologies are straightforward. Future work will help to validate and constrain these approaches, and especially the associated error bars.

The calculations for constraining the slope of a river system are relatively uncomplicated with a clear-cut application to ancient sandy river deposits. It is necessary to have good measurements of paleo river depth, median bed-material-load particle diameter, and the coarsest fraction of sediment carried in suspension. While each parameter can be measured in a variety of ways, spatial averaging of a considerable number of measurements reduces uncertainties. The use of three separate methods, both empirical (methods 1 and 2) and theoretical (method 3), provides a substantial check on internal consistency. These methods, when combined with other data obtained from sources such as bedform phase diagrams and hydraulic-geometry curves, as well as spatial and

TABLE 3.—*Estimation and RMS error of the measured reach-averaged slope using the suspension criteria method, for individual (not averaged) suspended load and slackwater samples and the average maximum flow depth. Estimation error represents the average value of each sample type for each river.*

River	Sample Type	Estimation Error (%)	RMS Error	Number of Samples
Niobrara	Suspended load	−30.0	4.1×10^{-4}	19
	Slackwater	−42.7	6.8×10^{-4}	6
North Loup	Suspended load	−77.5	1.2×10^{-3}	9
	Slackwater	−79.5	1.2×10^{-3}	6
Calamus	Suspended load	63.1	1.3×10^{-4}	12
	Slackwater	−6.6	1.6×10^{-3}	14

temporal variation in sediment-transporting conditions tied to flow depth, channel geometry, and particle sizes, yield a more robust and complete picture of the paleo flow conditions responsible for sediment deposition and preservation.

ACKNOWLEDGMENTS

Many thanks to Stephanie Davidson and Gregory Nadon for useful reviews that significantly strengthened the manuscript. We also thank Gregory Wilkerson and Maarten Kleinhans for reviewing an earlier version of the manuscript. Support for this project was provided from the National Science Foundation (EAR-0345366). Funding was also received from the AAPG Grant-in-Aid program, a Geological Society of America Graduate Student Research Grant, an International Association of Sedimentology Student Grant, and a Rocky Mountain Section SEPM Fluvial Sedimentology Award. We thank Laura Vietti, Douglas Jerolmack, Kyle Straub, Vivian Leung, and Joel Johnson for field collaboration.

SUPPLEMENTAL MATERIAL

The Lynds dataset, including measurements of particle diameter and flow depth from the North Loup, Niobrara, and Calamus rivers in Nebraska, U.S.A., as well as sample collection and processing methods, are available from JSR's data archive: http://sepm.org/pages.aspx?pageid=229.

NOTATION

The following symbols are used in this paper:

$\langle\rangle$	spatial averaging
b	bed-load-layer height
C_d	0.21 for separated flow, drag coefficient
D	particle diameter
D_{50}	median particle diameter
D_{50b}	bed-material load, median particle diameter
D_{95}	95TH percentile particle diameter
D_{95s}, D_{99s}	suspended load, 95th and 99th percentile particle diameter
D_{95sw}	slackwater, 95th percentile particle diameter
D_{max}	maximum percentile particle diameter
D_{maxs}	suspended load, maximum percentile particle diameter
D_*	dimensionless particle size
F	τ_b/τ_{sf}
g	acceleration due to gravity
h_d	mean dune height
H	flow depth
H_{bf}	bankfull flow depth
k	0.407, von Kármán's constant
λ	mean dune length
ν	kinematic water viscosity
R	submerged specific gravity, $R=\rho_s/\rho-1\cong 1.65$ for quartz
Re_p	particle Reynolds number
ρ_s	sediment density
ρ	fluid density
S	water-surface slope
τ_a^*	nondimensional shear stress
τ_b	total boundary shear stress
τ_{bf50}^*	nondimensional Shields number at bankfull flow
τ_{cr}	critical shear stress for initial motion
τ_d	form drag associated with a train of dunes
τ_{fd}	form-drag boundary shear stress
τ_{sf}	skin-friction shear stress
u_{sf}^*	skin-friction shear velocity
w_s	settling velocity
$w_{s(Dmaxs)}$	settling velocity of D_{maxs} of the suspended load
W_*	dimensionless settling velocity
$(z_o)_{sf}$	bed roughness from saltating sediment

REFERENCES

Allen, J.R.L., 1982, Sedimentary Structures: Their Character and Physical Basis, Volume 1: Amsterdam, Elsevier Publishers, 593 p.

Armitage, J.J., Duller, R.A., Whittaker, A.C., and Allen, P.A., 2011, Transformation of tectonic and climatic signals from source to sedimentary archive: Nature Geoscience, v. 4, p. 231–235.

Bagnold, R.A., 1966, An approach to the sediment transport problem from general physics: U.S. Geological Survey, Professional Paper P 422-I, 37 p.

Best, J.L., and Ashworth, P.J., 1997, Scour in large braided rivers and the recognition of sequence stratigraphic boundaries: Nature, v. 387, p. 275–277.

Bhattacharya, J.P., and MacEachern, J.A., 2009, Hyperpycnal rivers and prodeltaic shelves in the Cretaceous Seaway of North America: Journal of Sedimentary Research, v. 79, p. 184–209.

Bhattacharya, J.P., and Tye, R.S., 2004, Searching for modern Ferron analogs and applications to subsurface interpretation, *in* Chidsey, T.C., Jr., Adams, R.D., and Morris, T.H., eds., Regional to Wellbore Analog for Fluvial–Deltaic Reservoir Modeling: The Ferron Sandstone: American Association of Petroleum Geologists, Studies in Geology 50, p. 39–57.

Brownlie, W.R., 1981, Compilation of alluvial channel data: laboratory and field: W.M. Keck Laboratory of Hydraulics and Water Resources, Division of Engineering and Applied Science, California Institute of Technology, Pasadena, Report No. KH-R~43B, 37 p.

Dalman, R.A.F., and Weltje, G.J., 2008, Sub-grid parameterisation of fluvio-deltaic processes and architecture in a basin-scale stratigraphic model: Computers & Geosciences, v. 34, p. 1370–1380.

Davidson, S.K., and North, C.P., 2009, Geomorphological regional curves for prediction of drainage area and screening modern analogues for rivers in the rock record: Journal of Sedimentary Research, v. 79, p. 773–792.

Dietrich, W.E., 1982, Settling velocity of natural particles: Water Resources Research, v. 18, p. 1615–1626.

Duller, R.A., Whittaker, A.C., Swinehart, J.B., Armitage, J.J., Sinclair, H.D., Bair, A., and Allen, P.A., 2012, Abrupt landscape change post-6 Ma on the central Great Plains, USA: Geology, v. 40, p. 871–874.

Ferguson, R.I., and Church, M., 2004, A simple universal equation for grain settling velocity: Journal of Sedimentary Research, v. 74, p. 933–937.

Foreman, B.Z., Heller, P.L., and Clementz, M.T., 2012, Fluvial response to abrupt global warming at the Palaeocene/Eocene boundary: Nature, v. 491, p. 92–95.

Fredsøe, J., 1982, Shape and dimensions of stationary dunes in rivers: American Society of Civil Engineers, Journal of the Hydraulics Division, v. 108, p. 932–947.

Frings, R.M., and Kleinhans, M.G., 2008, Complex variations in sediment transport at three large river bifurcations during discharge waves in the river Rhine: Sedimentology, v. 55, p. 1145–1171.

Gabel, S.L., 1993, Geometry and kinematics of dunes during steady and unsteady flows in the Calamus River, Nebraska, USA: Sedimentology, v. 40, 237–269.

Guy, H.P., Simons, D.B., and Richardson, E.V., 1966, Summary of alluvial channel data from flume experiments, 1956–1961: U.S. Geological Survey, Professional Paper 462-I, 96 p.

Hajek, E.A., Huzurbazar, S.V., Mohrig, D., Lynds, R.M., and Heller, P.L., 2010, Statistical characterization of grain-size distributions in sandy fluvial systems: Journal of Sedimentary Research, v. 80, p. 184–192.

Heller, P.L., Dueker, K., and McMillan, M.E., 2003, Post-Paleozoic alluvial gravel transport as evidence of continental tilting in the U.S. Cordillera: Geological Society of America, Bulletin, v. 115, p. 1122–1132.

Jerolmack, D.J., Mohrig, D., and McElroy, B., 2006, A unified description of ripples and dunes in rivers, *in* Parker, G., and Garcia River, M., Coastal and Estuarine Morphodynamics: London, Taylor and Francis Group, p. 843–851

Jiminez, J.A., and Madsen, O.S., 2003, A simple formula to estimate settling velocity of natural sediments: Journal of Waterway, Port, Coastal and Ocean Engineering, v. 129, p. 70–78.

Julien, P.Y., 2010, Erosion and Sedimentation, Second Edition: Cambridge University Press, 371 p.

Kim, W., Paola, C., Swenson, J.B., and Voller, V.R., 2006, Shoreline response to autogenic processes of sediment storage and release in the fluvial system: Journal of Geophysical Research, v. 111, F04013.

Kleinhans, M.G., Wilbers, A.W.E., and ten Brinke, W.B.M., 2007, Opposite hysteresis of sand and gravel transport up- and downstream of a bifurcation during a flood in the River Rhine, The Netherlands: Netherlands Journal of Geoscience, v. 85, p. 273–285.

Laursen, E.M., 1958, The total sediment load of streams: American Society of Civil Engineers, Journal of the Hydraulics Division, Proceedings, v. 84, p. 1530-1–1530-36.

Leclair, S.F., 2002, Preservation of cross-strata due to the migration of subaqueous dunes: an experimental investigation: Sedimentology, v. 49, p. 1157–1180.

Leclair, S.F., 2010, Predicting preserved stratigraphy from dunebed topography after annual peak flows in a modern large river [abstract]: American Association of Petroleum Geologists, Annual Convention, Official Program, v. 19, p. 144.

Leclair, S.F., and Bridge, J.S., 2001, Quantitative interpretation of sedimentary structures formed by river dunes: Journal of Sedimentary Research, v. 71, p. 713–716.

Leclair, S.F., Bridge, J.S., and Wang, F.Q., 1997, Preservation of cross-strata due to migration of subaqueous dunes over aggrading and non-aggrading beds: comparison of experimental data with theory: Geoscience Canada, v. 24, p. 55–66.

Lynds, R.M., 2005, Fine-grained sediment in modern and ancient sandy braided rivers [unpublished Ph.D. Thesis]: University of Wyoming, Laramie, 163 p.
Lynds, R.M., and Hajek, E.A., 2006, Predictive model for reservoir compartmentalization in sandy braided river deposits: American Association of Petroleum Geologists, Bulletin, v. 90, p. 1251–1272.
McMillan, M.E., Angevine, C.L., and Heller, P.L., 2002, Postdepositional tilt of the Miocene–Pliocene Ogallala Group on the western Great Plains: evidence of late Cenozoic uplift of the Rocky Mountains: Geology, v. 30, p. 63–66.
Mohrig, D., 1994, Spatial evolution of dunes in a sandy river [unpublished Ph.D. Thesis], University of Washington, Seattle, 130 p.
Mohrig, D., and Smith, J.D., 1996, Predicting the migration rates of subaqueous dunes: Water Resources Research, v. 32, p. 3207–3217.
Mohrig, D., Heller, P.L., Paola, C., and Lyons, W.J., 2000, Interpreting avulsion process from ancient alluvial sequences: Guadalope–Matarranya system (northern Spain) and Wasatch Formation (western Colorado): Geological Society of America, Bulletin, v. 112, p. 1787–1803.
Nelson, J.M., and Smith, J.D., 1989a, Flow in meandering channels with natural topography, *in* Ikeda, S., and Parker, G., River Meandering: American Geophysical Union, Water Resources, Monograph 12, p. 69–102.
Nelson, J.M., and Smith, J.D., 1989b, Mechanics of flow over ripples and dunes: Journal of Geophysical Research, Oceans, v. 94, p. 8146–8162.
Nelson, J.M., McLean, S.R., and Wolfe, S.R., 1993, Mean flow and turbulence fields over two-dimensional bed forms: Water Resources Research, v. 29, p. 3935–3953.
Niño, Y., Fabian, L., and Marcelo, G., 2003, Threshold for particle entrainment into suspension: Sedimentology, v. 50, p. 247–263.
Paola, C., 1997, When streams collide: Nature, v. 387, p. 232–233.
Paola, C., and Borgman, L.E., 1991, Reconstructing random topography from preserved stratification: Sedimentology, v. 38, p. 553–565.
Paola, C., and Mohrig, D., 1996, Palaeohydraulics revisited: palaeoslope estimation in coarse-grained braided rivers: Basin Research, v. 8, p. 243–254.
Paola, C., Heller, P.L., and Angevine, C.L., 1992, The large-scale dynamics of grain-size variation in alluvial basins: 1, theory: Basin Research, v. 4, p. 73–90.
Parker, G., 1978, Self-formed straight rivers with equilibrium banks and mobile bed, part 2, the gravel river: Journal of Fluid Mechanics, v. 89, p. 127–146.
Parker, G., 2008, Transport of Gravel and Sediment Mixtures, Chapter 3, Sedimentation Engineering, *in* Garcia, M.H., ed., Processes, Measurements, Modeling and Practice: American Society of Civil Engineers, Manuals and Reports on Engineering, Practice no. 110, p. 165–252.
Riley, S.J., and Bryant, T., 1979, The relationship between settling velocity and grainsize values: Geologic Society of Australia, Journal, v. 26, p. 313–315.
Rubin, D.M., and McCulloch, D.S., 1980, Single and superimposed bedforms: a synthesis of San Francisco Bay and flume observations: Sedimentary Geology, v. 26, p. 207–231.
Smith, J.D., and Hopkins, T.S., 1972, Sediment transport on the continental shelf off of Washington and Oregon in light of recent current measurements, *in* Swift, D.J.P., Duane, D.B., and Pilkey, O.H., eds., Shelf Sediment Transport: Stroudsburg, Dowden, Hutchinson & Ross, p. 143–180.
Smith, J.D., and McLean, S.R., 1977, Spatially averaged flow over a wavy surface: Journal of Geophysical Research, v. 82, p. 1735–1746.
Topping, D.J., Rubin, D.M., Nelson, J.M., Kinzel, P.J., III, and Bennett, J.P., 1999, Linkage between grain-size evolution and sediment depletion during Colorado River floods, *in* Webb, R.H., Schmidt, J.C., Marzolf, G.R., and Valdez, R.A., eds., The Controlled Flood in Grand Canyon: American Geophysical Union, Geophysical Monograph, v. 110.
Whipple, K.X., Parker, G., Paola, C., and Mohrig, D., 1998, Channel dynamics, sediment transport, and the slope of alluvial fans: experimental study: Journal of Geology, v. 106, p. 677–693.
Whipple, K.X., and Trayler, C.R., 1996, Tectonic control of fan size: the importance of spatially variable subsidence rates: Basin Research, v. 8, p. 351–366.
Wiberg, P.L., and Rubin, D.M., 1989, Bed roughness produced by saltating sediment: Journal of Geophysical Research, Oceans, v. 94, p. 5011–5016.
Wilkerson, G.V., and Parker, G., 2011, Physical basis for quasi-universal relationships describing bankfull hydraulic geometry of sand-bed rivers: Journal of Hydraulic Engineering, v. 137, p. 739–753.
Yalin, M.S., 1977, Mechanics of Sediment Transport: Oxford, U.K., Pergamon Press, 298 p.
Yalin, M.S., 1992, River Mechanics, Oxford, U.K., Pergamon Press, 219 p.

Received 14 May 2013; accepted 17 July 2014.